Structural Characterization and Optimization of Antibody-Selected Phage Library Mimotopes of an Antigen Associated with Autoimmune Recurrent Thrombosis

Daniel S. Sem,*,‡ Brian L. Baker, Edward J. Victoria, David S. Jones, David Marquis, Lin Yu, Joshua Parks, and Stephen M. Coutts

La Jolla Pharmaceutical Company, 6455 Nancy Ridge Drive, San Diego, California 92121

Received March 30, 1998; Revised Manuscript Received July 7, 1998

ABSTRACT: The presence of high titers of anti-cardiolipin antibodies (ACA's) of autoimmune origin, which are known to bind to plasma β_2-glycoprotein I (aka apolipoprotein H), correlates clinically with autoimmune recurrent thrombosis. Soluble β_2-glycoprotein I binds to solid-phase ACA (immobilized on a surface plasmon resonance chip) with a K_d of 1.4 μM, but if the reactants are reversed and β_2-glycoprotein I is on the solid-phase support, then the K_d is 52 nM. This 27-fold difference in affinity reflects the avidity/entropic advantage obtained for an antibody binding to an antigen that is made multivalent because it is attached to a solid phase. A mimotope of this antigen, selected from a phage display peptide library screen with an ACA, has been shown to bind to solid-phase ACA as a phage, using surface plasmon resonance. This peptide is representative of the motif from 37 peptides obtained in a previously reported phage library screen with this ACA (*1*). A synthetic version of this peptide, referred to as P4, has the sequence: $A^1G^2P^3C^4I^5L^6L^7A^8R^9D^{10}R^{11}C^{12}P^{13}G^{14}$, and binds to its selecting antibody with a K_d of 42 nM. NMR data indicate that proline-13 is present in both cis and trans configurations, and that these two geometries dramatically affect the overall tertiary structure of the molecule. The peptide lacking this proline binds severalfold better to the ACA, consistent with at least one of these structures having low affinity for binding ACA. Replacement of the arginine-9 position with a proline decreases binding affinity to ACA 10-fold. Another phage library-selected peptide has a proline in position 9, but also has a leucine in position 5, instead of isoleucine. Since its affinity for ACA is nearly as good as that for peptide P4, the phage library screening must have selected for a non-β-branched amino acid in this position to compensate for the adverse effects of the arginine-9 to proline-9 substitution. The solution structure of a modified version of the antibody-selected phage peptide P4 with the central proline was determined. This peptide has one turn comprised of Ala-Pro-Asp-Arg, with the proline peptide bond in the cis configuration, and another turn that contains the disulfide and adjacent residues. If the disulfide is replaced by a thioether, and the central proline by an α-methyl proline, in an attempt to make the peptide more biologically stable, there is little adverse effect on affinity for ACA. The thioether bond/turn is fairly well defined with a Cα to Cα separation of 4.9 ± 0.8 Å. The α-methyl proline adopts the trans configuration, and this central Ala-(α-methyl-Pro)-Asp-Arg turn adopts a distorted type I turn conformation with a probable i to $i+3$ hydrogen bond. Modeling studies suggest that the proline peptide bond configuration switched from cis to trans in the presence of the α-methyl group on proline because of steric hindrance with the β-carbon of the preceding residue. Overall, this peptidomimetic molecule is structurally very similar to the peptide with natural amino acids, with an rmsd difference of only 1.37 Å, when comparing backbone atoms.

The presence of autoantibodies against a complex between cardiolipin and β_2GPI[1] protein (*2*, *3*) is associated with thromboembolic events, stroke, recurrent spontaneous abortion, thrombocytopenia, and fetal death (*4*, *5*). β_2GPI is a 50 kDa plasma glycoprotein that was first isolated in 1961 (*6*). It is present at approximately 4 μM (200 μg/mL) in serum, but 40% is bound to lipoproteins (*7*). β_2GPI binds to the anionic surface of cardiolipin through positively charged residues, and after binding acquires higher affinity for autoantibodies. It is thought that cardiolipin enhances antibody affinity by either inducing a conformational change in β_2GPI that results in better presentation of the epitope to pathogenic antibodies or presenting β_2GPI antigen in a high-density ordered array to the antibodies, thus increasing their affinity of interaction through avidity (*8*, *9*).

* To whom correspondence should be addressed. Phone: 619-452-6600. FAX: 619-626-2845.

‡ Present address: Triad Biotechnology, Inc., P.O. Box 3503, Rancho Santa Fe, CA 92067.

[1] Abbreviations: β_2GPI, β_2-glycoprotein I; ACA, anti-cardiolipin antibody; NHS, *N*-hydroxysuccinimide; EDC, *N*-ethyl-*N*′-(3-diethylaminopropyl)carbodiimide; CM5, carboxymethylated dextran-5; PBS, phosphate-buffered saline; BGG, bovine gamma globulin; HEPES, *N*-(2-hydroxyethyl)piperazine-*N*′-2-ethanesulfonic acid; EDTA, ethylenediaminetetraacetic acid; HBS, HEPES-buffered saline; pfu, plaque forming unit; FITC, fluorescein isothiocyanate; TFA, trifluoroacetic acid; NMR, nuclear magnetic resonance; DQF-COSY, double quantum filtered correlation spectroscopy; NOESY, nuclear Overhauser enhancement spectroscopy; ROESY, rotating frame Overhauser enhancement spectroscopy; TOCSY, total correlation spectroscopy; rmsd, root-mean-square deviation.

10.1021/bi9807207 CCC: $15.00
Published on Web 10/30/1998

Although there have been various studies suggesting where the epitope(s) may reside (*10*, *11*), its exact location in the 326 amino acid β_2GPI (*12*) is still not clearly defined. The relevant epitope in β_2GPI, or a mimic of it, might be used to construct a B-cell Toleragen (*13*), to down-regulate those B lymphocytes that produce the pathogenic antibodies in antibody-mediated thromboses. Such a drug is needed because current treatments with anticoagulation therapy are either not adequate or require long-term medication (*14*, *15*). Although general reduction in immunoglobulin levels using immunoglobulin therapy (IVIG) has shown some promise (*16*), the specific removal of pathogenic immunoglobulins using an antigen mimic of the β_2GPI epitope tethered to a multivalent platform, as a Toleragen, is a more targeted approach.

In the absence of specific knowledge regarding an epitope, mimics can be identified by screening phage peptide libraries (*17*) using autoantibodies against the native antigen (*18*). The best mimics of antigens, discovered through phage library screening, tend to be cyclic peptides, since they offer the entropic advantage of adopting a conformationally constrained state prior to binding antibody (*19*, *20*). Although it is well established that the antigenic regions on proteins are flexible and solvent-accessible (*21*−*23*), the best peptide mimotopes of protein antigens are themselves highly structured (*24*). Cyclization may be essential for successful mimotope selection, since linear peptides usually are very flexible and unstructured (*25*). Furthermore, successful mimicking of a protein antigen seems to require at least 10 amino acids (*26*). Once a peptide mimotope is discovered, before it can be useful as a drug, it must be stabilized against proteolysis so its in vivo activity is prolonged, and also so that it cannot be presented as a T-cell epitope, which would generate an immune response. Construction of an antigen mimotope such as this is a prelude to building a Toleragen drug, and these studies are in progress.

Strategies are being developed for the structure-guided design of mimetics of lead peptides, and there have been some successes reported (*27*−*29*). Notable advances include the substitution of thioether bonds in place of disulfides (*28*, *30*) and the use of α-methyl proline to stabilize turns. We describe here the selection and peptidomimetic optimization of an autoantibody-selected phage-displayed peptide that mimics the antigen targeted by ACA autoantibodies.

MATERIALS AND METHODS

Reagents. CM5 chips, NHS, and EDC were from Biacore. Haptoglobin is a protein containing the short consensus repeat (sushi) motif found in β_2GPI, and is used here as a negative control. It is human phenotype 1-1 protein, from Sigma. Purified human β_2GPI is from Alexis, and nonimmune human IgG is from Zymed. Recombinant β_2GPI was expressed with a hexa-histidine tail in Tn5 cells using the *baculovirus* system (*31*). It was purified from the supernatant with a nickel-chelation affinity column (Qiagen). Protein concentrations were determined with the Bradford assay (Biorad).

Peptide Discovery and Synthesis. The P2 and P4[2] peptides were derived from a phage library screen (*32*) carried out with an anti-cardiolipin antibody (ACA) from patient #6501 (Marquis and Victoria, unpublished results). The library contained sequence combinations that included AGPC-$(X)_7$CPG, where X represents the randomly varied positions. It was constructed in fUSE5, and panning was done essentially as described previously (*33*). Phage containing peptide P4 were amplified and purified for BIAcore studies.

Peptides P1 through P5 were synthesized using standard Fmoc protocols (*34*). They were all prepared from Fmoc amino acids (Novabiochem) using an Advanced ChemTech Model 357 Peptide Synthesizer, typically on a scale of 0.15 mmol using *N*-α-Fmoc gly Wang resin (Novabiochem). One hour acylations of the piperidine-deblocked, resin-bound peptides were carried out twice with a 6-fold mole excess of Fmoc amino acid activated *in situ* with the coupling reagents 1-hydroxybenzotriazole (Sigma) and 1,3-diisopropylcarbodiimide (Aldrich). Following the final coupling and deblocking step, the methanol-washed, vacuum-dried resin beads with the synthesized peptides were deprotected and cleaved from the resin using trifluoroacetic acid/phenol/ethanedithiol/thioanisole/water (10:0.75:0.25:0.5:0.5, v/w/v/v/v) for 3 h. The crude peptides were purified by preparative HPLC using a Vydac C18 column at a flow rate of 10 mL/min using a linear gradient of 15−45% B over 60 min (buffer A, 0.1% trifluoroacetic acid/water; buffer B, 0.1% trifluoroacetic acid/acetonitrile). The peptides showed the correct mass by electrospray mass spectrometry, and purity >95% by analytical HPLC. The LJP 685 peptide also required the synthesis of (*S*) α-methyl proline, and the formation of a thioether bond in place of the disulfide. The complete synthesis is described elsewhere (*35*).

FITC-P5 was prepared by reacting P5 peptide with fluorescein isothiocyanate isomer I from Aldrich. The peptide (10 mg, 6.7 mmol) was dissolved in 10 mL of a sodium carbonate solution in ACN/water (1:1), followed by the addition of fluorescein isothiocyante isomer I (2.8 mg, 6.7 mmol). The resulting solution was stirred at room temperature, and the reaction was followed by C18-HPLC [5−50% B at 1 mL/min over 20 min, where A was 0.1% (v/v) TFA in H_2O and B was 0.08% (v/v) TFA in ACN]. After the reaction was done (about 5 h), TFA was added to neutralize the solution, and the solvents were removed under vacuum. The crude product was purified using preparative C18 HPLC eluted at 10 mL/min with a linear gradient from 30 to 50% B over 40 min. FITC-P5 was obtained as a yellow powder after lyophilization: 3.4 mg, 29% yield; analytical RP-HPLC (5−50% B at 1 mL/min over 20 min): t_R 19.35 min; purity 100%; MS (ESI): *m*/*e* (M+1) calculated for $C_{73}H_{101}N_{19}O_{20}S_3$ 1662, observed 1662.

Purification of Anti-Cardiolipin Antibody (*ACA*) *6501 from Serum*. ACA 6501 is the antibody used in the binding studies reported in this paper and in the screening of the peptide phage libraries that produced peptides P2 and P4. It is from a Caucasian, female, 63-year-old patient with a history of venous thrombosis, aortic valve replacements, recurrent miscarriages, and a diagnosis of lupus-type syndrome. This patient had a GPL (IgG phospholipid assay) score of 151, as determined in a standard solid-phase ACA ELISA at a

[2] After *in situ* removal of the signal sequence, the amino-terminal sequence of pIII is ADGAGPCILLARDRCPGAA... (Marquis and Cockerill, unpublished results), with the inserted sequence corresponding to peptide P4 underlined. The peptide P4 phage was provided by Keith Cockerill.

plasma dilution of 1:50 (*36*). The purification method employed follows two previously published reports (*2, 37*) and uses cardiolipin-containing, multilamellar dispersions with bound β_2GPI to affinity-bind ACA. In a 25 mL round-bottom flask, a mixture of cardiolipin, cholesterol, and dicetyl phosphate (10:15:2, by mol) was dried using a rotary evaporator (Büchi Rotavap, Switzerland), and was then swollen in 2 mL of 0.96% (w/v) NaCl after mild vortexing and incubation for 1 h at 37 °C (final cardiolipin concentration was 1 mM). One milliliter of the liposome suspension was transferred to a clean flask to which 4 mL of ACA serum previously centrifuged at 600*g* was added. The mixture was incubated with agitation at medium speed in an orbital shaker for 48 h at 4 °C, and then for an additional 2h at 37 °C. Twenty milliliters of cold Tris-buffered saline, pH 7.4 (TBS), was added, and the mixture was transferred to a 50 mL polycarbonate centrifuge tube and centrifuged at 27000*g* for 15 min at 4 °C. The precipitate was washed 3 times with 25 mL of cold 0.96% NaCl using the same centrifugation conditions. The pellet was dissolved in 1 mL of 2% (w/v) solution of *n*-octyl β-D-glucopyranoside in TBS and applied to a 0.6 mL protein A cross-linked agarose (Repligen Corp., Cambridge, MA) column which had been prewashed with 15 times bed volume of 1 M acetic acid and equilibrated with 15 times bed volumes of TBS. The antibody−protein A/agarose column was washed with 40 times bed volume of 2% octyl glucopyranoside to remove lipids, followed by extensive washings with TBS until the optical density of the eluate at 280 nm approached base line. The bound antibody was eluted with 1 M acetic acid. One milliliter fractions were collected, and were neutralized immediately with 3 M Tris and kept in an ice bath. Based on $A_{280\ nm}$ readings, fractions containing antibody were pooled, concentrated, and washed 4 times with TBS in Centricon-30 concentrators (Amicon) per the manufacturer's protocol. The average yield obtained was 750 μg of antibody from 4 mL of serum from patient 6501. The purified antibody was tested for ACA activity and checked for purity by SDS−PAGE and Western blotting with rabbit anti-β_2GPI.

Surface Plasmon Resonance. All experiments were done on a BIAcore 2000 instrument at 25 °C with a flow rate of 10 μL/min. Chip equilibration and binding studies were done with degassed HBS buffer, which consists of 0.01 M HEPES, pH 7.4, 0.15 M NaCl, 3 mM EDTA, and 0.005% (v/v) surfactant P20. Coupling of protein ligands through their amino groups to the CM5 chip is done by flowing 40 μL of 0.05 M NHS/0.2 M EDC over the chip (*38*) to activate the chip, followed by exposure to the appropriate protein ligand. In the experiments with antibody on the chip, ACA 6501 was immobilized by flowing 50 μL of a 50 μg/mL ACA 6501 solution in 10 mM acetate, pH 4.8, over the NHS-activated CM5 chip. The titration was then done by repeatedly flowing 30 μL solutions of purified human β_2GPI, or recombinant β_2GPI(His)$_6$, over the ACA 6501 chip at different concentrations, and regenerating the chip between binding cycles with 50 μL of 0.1 M glycine hydrochloride (pH 2.1), 0.1 M NaCl. Response plateau values were taken at 190 s, after binding had reached equilibrium (Figure 1B,D), and these values were plotted versus the concentrations of β_2GPI (Figure 1A,C) that were flowed over the chip. Dissociation constants were obtained by fitting the titration curves in Figure 1A,C,E to eq 1:

$$R_{eq} = \frac{R_{max}C}{K_d + C} \quad (1)$$

where R_{eq} is the measured BIAcore response plateau value (in response units) once equilibrium is reached, K_d is the equilibrium dissociation constant, C is the concentration of analyte flowing over the chip, and R_{max} is the maximum BIAcore response for a chip that has its immobilized ligand fully saturated with analyte. Recombinant β_2GPI(His)$_6$ or haptoglobin was immobilized by flowing 70 μL of a 25 μg/mL β_2GPI(His)$_6$ solution in 10 mM acetate, pH 4.8, over the NHS-activated CM5 chip. The titration was done as described above, but this time with antibody ACA 6501 flowed over the chip. Data analysis was also as described above, but since the approach to binding equilibrium was so slow, it was necessary to extrapolate to R_{eq} by fitting the association curves in Figure 1F to eq 2:

$$R_t = R_{eq}(1 - e^{-k_s(t-t)_o}) + R_o \quad (2)$$

where R_t is the measured BIAcore response at time t, R_{eq} is the same as in eq 1, t is time, t_o is initial time, k_s is an apparent association constant ($k_s = k_aC - k_{dis}$, where k_a is the association constant, C is the analyte concentration, and k_{dis} is the dissociation constant), and R_o is a response offset.

Binding experiments with phage-(peptide P4) were done with a chip that had ACA 6501 immobilized in flow cells 1 and 3, and nonimmune human IgG immobilized in flow cell 2. Immobilization was done by flowing 50 μL of a 50 μg/mL solution of the appropriate antibody in 10 mM acetate, pH 4.8, over the NHS-activated CM5 chip. The phage used in the titration contains peptide P4 on the amino terminus of the pIII protein.[2] After equilibration of the antibody chip in HBS buffer, 100 μL of a solution containing 2×10^{11} pfu/mL of (peptide P4)-phage in HBS was injected, followed by reequilibration with HBS for 240 s, then a second injection of 100 μL of a solution containing 2×10^{12} pfu/mL of (peptide P4)-phage in HBS, and finally another equilibration with HBS (Figure 2).

Fluorescence Polarization. Fluorescence polarization experiments were carried out on a Beacon (PanVera) system, with all samples in a PBS/BGG buffer consisting of 9.3 mM potassium phosphate, 2.7 mM KCl, 138 mM NaCl, 0.02% sodium azide, and 100 μg/mL bovine gamma globulin (PanVera) at pH 7.4. The concentration of FITC-P5 peptide was determined based on $A^{1\%}_{493\ nm} = 1538$, and a molecular weight of 389 for FITC (*39*). Peptide FITC-P5 at 1 nM was titrated with ACA 6501 (Figure 3A). The dissociation constant was obtained by fitting the data in Figure 3A to

$$Y = Y_L + \frac{Y_H - Y_L}{1 + K_d/A} \quad (3)$$

where A is the concentration of ACA 6501, K_d is the dissociation constant for ACA 6501 binding to FITC-peptide, Y is the observed mP (milli-polarization) value, Y_L is the mP value at zero ACA 6501 concentration, and Y_H is the mP value for peptide that is fully bound to ACA 6501. The value of K_d obtained in this way should be multiplied by 2 to get the dissociation constant for binding of FITC-peptide to a single antibody binding site. Competitive inhibition constants for unlabeled peptide binding to ACA 6501 were

obtained by incubating a FITC-P5 peptide/ACA 6501 complex in PBS/BGG as above, but in the presence of an unlabeled peptide at various concentrations. After 15 min of equilibration time, the mP value was recorded, and plotted as a function of inhibitor concentration (Figure 3B). The apparent inhibition constant (K_i') was obtained from a fit of these data to

$$Y = Y_H' + \frac{Y_L - Y_H'}{1 + K_i'/I} \quad (4)$$

where Y is the observed mP value, I is the concentration of unlabeled peptide inhibitor, Y_H' is the mP value in the absence of inhibitor, and Y_L is the mP value in the presence of enough inhibitor to fully displace the FITC-peptide from the antibody. To get the true K_i from K_i', it is necessary[3] to divide by $(1 + A/K_d)$, where A and K_d are from eq 3. The A/K_d ratio is 0.757 in these experiments. Figure 3B shows a representative titration curve, and K_i values for all peptides studied are summarized in Table 1. Free energy changes resulting from substitutions made to the peptides (Figure 4) were obtained from ratios of the K_i values in Table 1 (*41*).

NMR Spectroscopy. Peptide samples were 8−20 mg/mL in water containing 10% D_2O. The pH of the peptide samples in Figure 5 was 3.5, while the pH of samples used for structure determination was 5.8 (with some data at pH 3.5 for comparison) for peptide P1, and 4.5 for LJP 685. All NMR experiments were carried out on Bruker AC300 or AC500 spectrometers with the carrier on HOD at 298 K, with additional spectra at 5−10 °C for peptides P1 and LJP 685. In the temperature coefficient experiments (Figure 6D), temperature calibration was done with methanol, based on differences in chemical shifts between methyl and hydroxyl protons. Quadrature detection was with time-proportional phase incrementation (*42*, *43*). Spin system assignments were made from DQF-COSY (*44*) and TOCSY (*45*) spectra, and connectivities and distance constraints for structure calculations were obtained from NOESY (*46*) and ROESY (*47*) spectra. All spectra had 2048 data points in $\omega 2$, and a spectral width of 4000 Hz (DQF-COSY and NOESY) or 5555.55 Hz (TOCSY and ROESY). The TOCSY used a MLEV17 spin lock for 50 ms, the ROESY experiments had mixing times of 200 and 300 ms, and the NOESY experiments had mixing times of 100 and 200 ms. There were 1024 increments in $\omega 1$ with 16 scans per increment for the DQF-COSY and TOCSY, and 512 increments in $\omega 1$ with 32 scans per increment for the NOESY and ROESY. Spectra were processed on the spectrometer, or with nmrPipe (*48*). Processing was done using shifted sine bells in both dimensions, and water was removed using a low-pass filter (*49*). Deuterium exchange rates were measured for peptide P1 by lyophilizing 10 mg from pH 3.5 water, then resuspending in D_2O prechilled to 5 °C, and measuring 1D spectra (16 scans, 2048 data points) at 12 °C at regular intervals. Signal intensities were fitted to a single-exponential decay or a double-exponential decay if DQF-COSY data indicated there was peak overlap. Protection factors (Figure 6C) were then calculated with standard methods (*50*).

[3] The full derivation of this and related equations will be presented elsewhere (*40*).

Structure Calculation for Peptide P1. Since molecular mechanics calculations can compress structures (*51*−*53*), and this effect is likely to be more dramatic with peptides because side chains are more solvent-exposed, structures were calculated using just distance geometry calculations. The structure of peptide P1 was calculated with DGII (MSI), using 14 sequential and 7 medium- to long-range NOE and ROE distance constraints (Figure 7A), and one dihedral constraint. Distance constraints were grouped as strong, medium, and weak, corresponding to distances up to 2.7, 3.3, and 5.0 Å, respectively. Bounds generation and triangle smoothing were done, followed by embedding using prospective metrization, with an ω wobble of 10° allowed for peptide bonds. Simulated annealing was done with an initial energy of 800 kcal, a mass of 1000 g/mol, and a step size of $3.2e^{-13}$ s, with 10 000 steps, and the maximum temperature was 200 K. Of the 50 structures generated, the best 15 were chosen (Figure 7B) based on having the lowest final error in the objective function, with the structure closest to the centroid shown in Figure 7C.

Structure Calculation for Peptide LJP 685. The structure of LJP 685 was calculated (Figure 8, white carbons) using DGEOM[4] with 10 sequential and 5 medium- to long-range ROE constraints. In the embedding step, triangle inequality bound smoothing was followed by metric matrix selection of trial interatomic distances between upper and lower bounds. Following the embedding step, two conjugate gradient minimization steps were performed where an error function (similar to potential energy) was minimized. To improve convergence and conformational sampling, a molecular dynamics step was included between these minimization steps. In the molecular dynamics, initial velocities were assigned to all atoms by a Boltzmann distribution about the initial temperature of 0.05 (arbitrary units). The temperature used for the bulk of the simulation was 0.05, and was reset every 100 steps by reassigning atom velocities based on a Boltzmann distribution around the temperature of 0.05. Dynamics were run with a step size of 0.05 (analogous to time, but in arbitrary units) for a total of 5000 steps. The 100 structures generated in this manner were then subjected to cluster analysis. Structures were grouped into structurally related families using COMPARE,[5] which clusters using a Jarvis-Patrick clustering routine.

Modeling. All minimizations were done with the AMBER force field (*54*) (as implemented in HyperChem), with conjugate gradient optimization. A minimized structure of LJP 685 was prepared from the DGEOM calculated structure of peptide P1 in Figure 7C, for the purpose of modeling the effect of changing the geometry of the proline-8 peptide bond from trans to the cis geometry observed in peptide P1. LJP 685, with trans α-methyl proline-8, was minimized in a 15 Å box of 450 water molecules (Figure 9C, left side). The cis isomer of LJP 685 was then modeled starting from the solution structure of peptide P1 (Figure 7C) by keeping proline-8 cis, and modifying it everywhere else to have the same atomic configuration as LJP 685, allowing only

[4] DGEOM95 was written by J. M. Blaney, G. M. Crippen, A. Dearing, J. Scott Dixon, and D. C. Spellmeyer, and is distributed by Quantum Chemistry Program Exchange (Bloomington, IN) as QCPE590.

[5] COMPARE was written by J. M. Blaney, and is distributed by Quantum Chemistry Program Exchange (Bloomington, IN) as part of QCPE590.

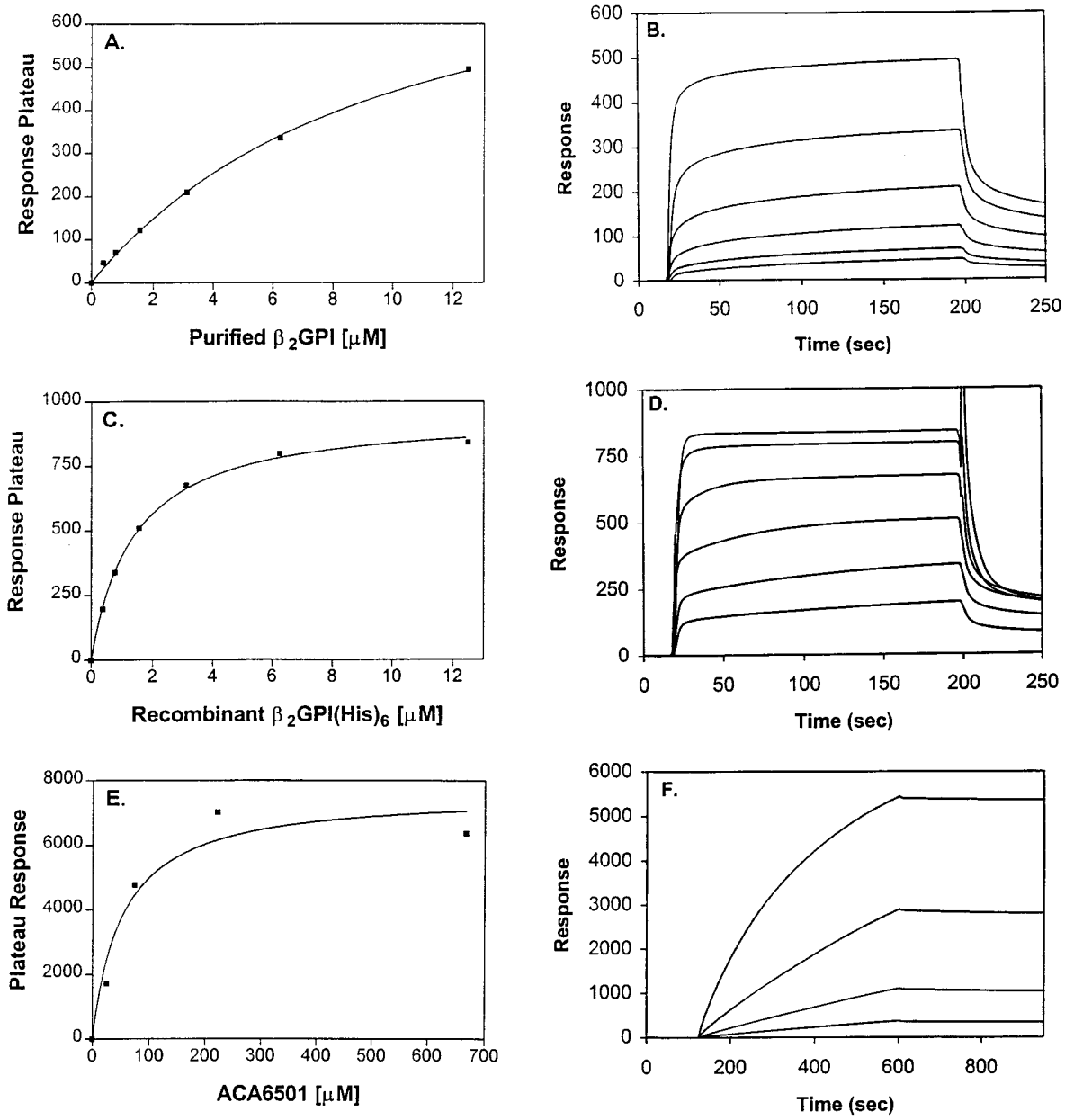

FIGURE 1: Panels A, C, and E show plots of BIAcore response plateau values for the titrations in Panels B, D, and F, respectively. BIAcore titration of ACA 6501 on the CM5 chip with (B) purified β_2GPI (0.0, 0.39, 0.78, 1.56, 3.12, 6.25, 12.5 μM) or (D) recombinant β_2GPI (0.0, 0.39, 0.78, 1.56, 3.12, 6.25, 12.5 μM). The reverse titration was carried out with recombinant β_2GPI on the CM5 chip and ACA 6501 (at 0.0, 74.1, 222, 667 μM) in the flow (F).

minimal changes in geometry relative to the starting peptide P1 structure. This structure was then minimized in water (as for LJP 685), with the methyls on α-methyl proline-8 and the preceding alanine-7 excluded from the calculation. This was followed by a minimization of just these two methyl groups, and then by a minimization of all atoms (Figure 9C, right side).

RESULTS

Characterization of Antigen and Antibody with Surface Plasmon Resonance Binding Studies. ACA 6501 is an affinity-purified antibody from a patient with a history of venous thrombosis. ACA 6501 attached to a BIAcore CM5 chip binds to purified native β_2GPI with a K_d of 9.8 ± 0.8 μM and a plateau response of 878 ± 39 response units (Figure 1A,B). The K_d for ACA 6501 binding to soluble recombinant *baculovirus*-expressed β_2GPI is 1.38 ± 0.08 μM, with a plateau response of 955 ± 16 response units (Figure 1C,D).[6] In contrast, if the recombinant β_2GPI is attached to a CM5 chip, the apparent affinity for ACA 6501 increases to a dissociation constant of 52 ± 23 nM (Figure 1E,F), because of avidity effects. As expected based on these relative affinities, dissociation of the antibody−antigen complex is slower with β_2GPI on the chip (Figure 1F) than with antibody on the chip (Figure 1B,D). Dissociation constants for solid-phase β_2GPI binding to ACA's from two other patient's sera (ACA 6641 and ACA 6626) were 55 and 62 nM. As a technical note, the type of equilibrium analysis of BIAcore data we have used avoids many of the

[6] The baculovirus viral construct containing the β_2GPI(His)$_6$ gene was prepared from a cDNA clone of β_2GPI provided by Steve Krilis, The St. George Hospital, Kogarah, Australia. The cloning and preparation of this protein are reported elsewhere (*31*).

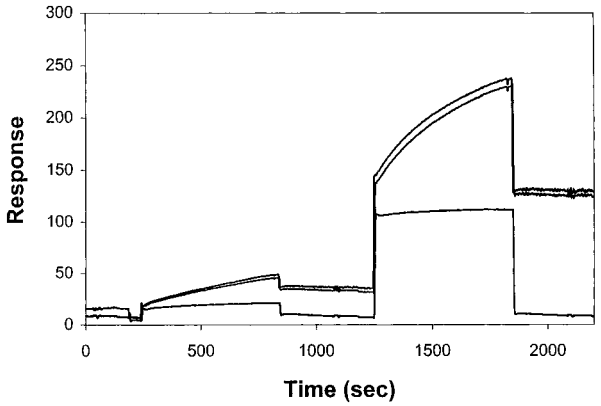

FIGURE 2: BIAcore titration of ACA 6501 on the CM5 chip with (peptide P4)-phage. First injection is with 2×10^{11} pfu/mL phage, and the second is with 2×10^{12} pfu/mL. Flow cells 1 and 3 (top two lines) have ACA 6501 immobilized on a CM5 chip, while flow cell 2 (bottom line) has normal human IgG (Zymed) immobilized.

artifacts due to kinetic mass transport effects (*55*, *56*). Since thermodynamic equilibrium constants are dependent only on initial and final states, how the approach to equilibrium is affected by mass transport effects is not a concern.

Direct Confirmation of Antibody Binding to a Phage-Bound Mimotope Peptide. ACA 6501 was used in the phage library screen that produced the P4 peptide (Marquis and Victoria, unpublished results). To verify the antibody−peptide binding that implicitly must have occurred for the selection to have worked, binding to ACA 6501 on a CM5 chip was monitored (Figure 2). A significant 25 unit change in response was detected above background binding to nonimmune human IgG at a (peptide-P4) phage concentration of 2×10^{11} pfu/mL, while a change of 120 response units was observed at 2×10^{12} pfu/mL. Once bound, no significant dissociation of peptide-phage was detected, as expected for a high affinity and avidity interaction. Since there are multiple copies of peptide P4 per phage, the apparent binding affinity for antibody will be higher because of avidity.

Peptide Affinities for ACA 6501. Affinities were measured using fluorescence polarization, monitoring the increase in polarization as FITC-P5 is titrated with ACA 6501 (Figure 3A), or by displacing FITC-P5 with unlabeled peptide and monitoring the decrease in polarization (Figure 3B). Dissociation constants are summarized in Table 1. The energetic consequences of changes made to the peptide sequences, calculated from the dissociation constants, are summarized in Figure 4. Modification of the amino terminus is very detrimental (P5 versus FITC-P5), as is the introduction of a proline in place of the arginine in the center of the peptide (P3 versus P4). Isoleucine, a β-branched amino acid, after the first cysteine is disfavored relative to leucine (P2 versus P3). Removal of the proline on the carboxy-terminal end of the molecule is advantageous (P4 versus P5). The attempt to make peptide P5 more metabolically stable, by introducing a thioether in place of the disulfide, replacing the central proline with an α-methyl proline, and terminating with the carboxamide of the last cysteine, had little adverse effect on the binding affinity for ACA 6501 (LJP 685 versus P5).

Preliminary Structural Characterization of Peptides. Peptide P2 (lacking alanine-1) has prolines flanking the cysteines that form the disulfide turn. The DQF-COSY spectrum of this peptide shows twice the number of cross-peaks in the fingerprint region (Figure 5A) as the spectrum of the same peptide that lacks the proline at the carboxy-terminal end of the molecule (Figure 5B). Thus, the carboxy-terminal proline is apparently present in both cis and trans configurations, which both have very different three-dimensional structures, based on the large chemical shift differences.

In addition to the solution structure of peptide P1 (*vide infra*), other data relating to structure were obtained (Figure 6). Chemical shift deviations from random coil values (Figure 6A,B) were not large, except for alanine-7, which showed the CαH deviation typical of a helical region. Protection factors and temperature coefficients provide no

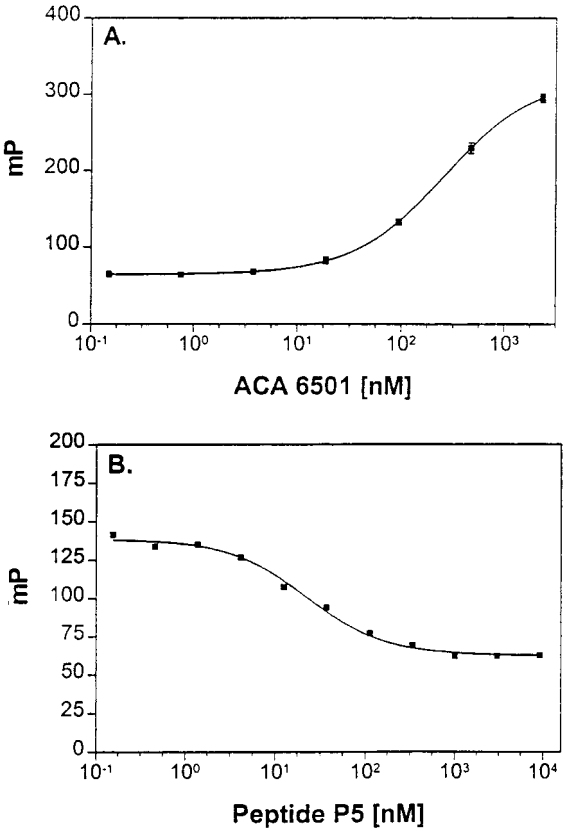

FIGURE 3: (A) Fluorescence polarization titration of 1.0 nM FITC-P5 with ACA 6501 at 2.35 μM, 470 nM, 94.0 nM, 18.8 nM, 3.76 nM, 0.752 nM, and 0.150 nM. Each data point represents the mP reading after zeroing on PBS/BGG buffer with ACA 6501, adding FITC-P5, and then waiting 15 min. (B) In a similar manner, FITC-P5/ACA 6501 complex was incubated with the peptide P5 inhibitor at concentrations of 9.12 μM, 3.02 μM, 339 nM, 112 nM, 37.2 nM, 12.6 nM, 4.17 nM, 1.38 nM, 0.457 nM, or 0.155 nM.

Table 1: Peptide Naming Convention and Dissociation Constants for Binding to ACA 6501, As Determined Using Fluorescence Polarization

peptide	name	K_i (nM)
GPCLILAPDRCG	P1	ND[a]
AGPCLLLAPDRCPG	P2	96.3 ± 0.9
AGPCILLAPDRCPG	P3	404 ± 1
AGPCILLARDRCPG	P4	42.5 ± 0.9
GPCILLARDRCG	P5	15.9 ± 0.5
(FITC-P5)	FITC-P5	512 ± 1
GP(hC)ILLAP^{Me}DRC-NH_2	LJP 685	23.7 ± 0.9

[a] Peptide P1 is a ca. 2-fold better inhibitor than P2 based on competitive ELISA results (Victoria and Hayag, unpublished results).

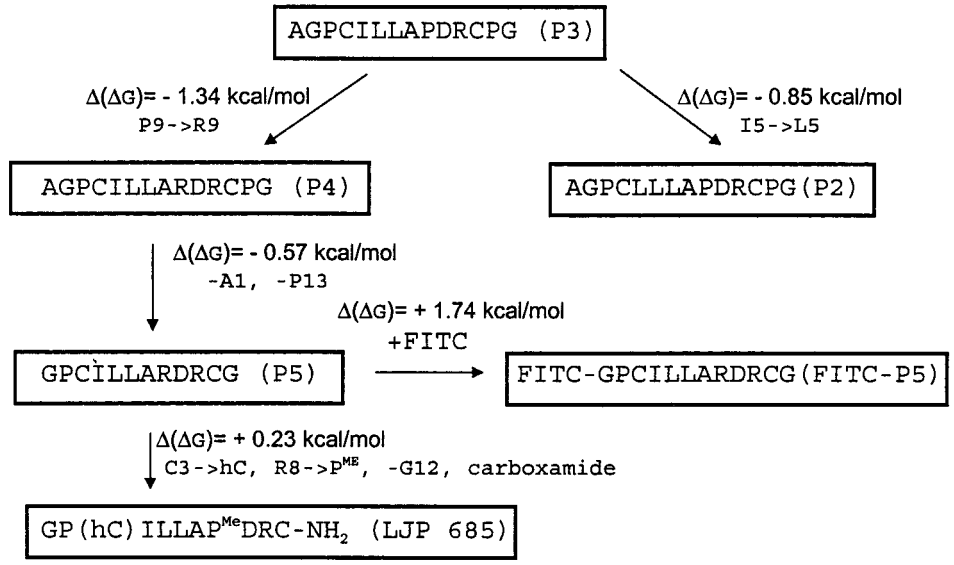

FIGURE 4: Free energy changes for various modifications to the original P4 peptide, based on binding constants obtained with competitive FP binding studies.

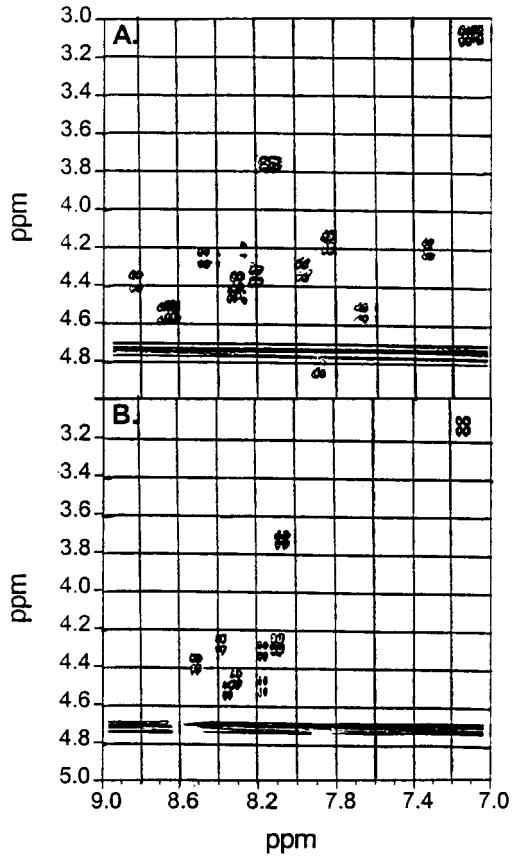

FIGURE 5: Effect of carboxy-terminal proline on the fingerprint region of the DQF-COSY spectrum of peptide P2 (with the amino-terminal alanine removed). (A) Spectrum of GPCLLLAPDRCPG. (B) Spectrum of GPCLLLAPDRCG.

compelling evidence for hydrogen bonding in peptide P1 (Figure 6C,D). Temperature coefficients for LJP 685 also showed no evidence of any hydrogen bond formation (data not shown). Most of the NOEs and ROEs observed in peptide P1 (Figure 7A) and LJP 685 are in the proline turn region. Peptide P1 showed all negative NOEs, except for the amide of glycine-12, which was positive, indicating that it is more flexible than the other residues. This is reflected in the structure shown in Figure 7B,[7] where the disordered carboxy terminus is shown in the center of the molecule, pointing out of the page.

Solution Structures of Peptide P1 and LJP 685. The solution structure of peptide P1 is fairly well-defined, with an average all-atom rmsd of 2.13 ± 0.22 Å, for the 15 structures out of 50 with the lowest error in the objective function. The average all-atom rmsd for all 50 structures is 2.93 ± 0.84 Å. For comparison, the structure of peptide P1 was also calculated using DGEOM.[4] There were essentially no differences in the structures obtained using these two different distance geometry algorithms (data not shown). Although the geometry around the glycine-1/proline-2 peptide bond could not be determined unambiguously because of overlap in the NMR spectra, the alanine-7/proline-8 peptide bond is clearly cis. Although NOEs to alanine-7 αH could not be detected because of spectral overlap with water, an NOE was observed between the alanine-7 NH and the proline-8 αH, while no NOE was observed between the alanine-7 βH and the proline-8 αH. Furthermore, the average objective function/energy for structures calculated with a trans geometry was 5 times higher than that with a cis geometry.

LJP 685 also appears to be a fairly structured peptide, since cluster analysis of all 100 structures generated by DGEOM produced 1 major family of 63 structures at an rmsd clustering cutoff of 5.08 Å. This family of 63 LJP 685 structures had an average all-atom rmsd of 3.04 ± 0.43 Å for all pairwise comparisons of structures. The 15 best structures had an all-atom rmsd of 2.82 ± 0.29 Å. The centroid of this family of LJP 685 structures is shown in Figure 8 (white carbons) overlayed on top of the centroid structure for peptide P1 (green carbons). The rmsd difference between the centroid structures for LJP 685 and peptide P1 is 1.37 Å, considering only backbone atoms (carbonyl carbon, α-carbon, amide nitrogen, and the disulfide/thioether cross-link). The thioether and α-methyl proline turn regions are

[7] Computational results were obtained using software programs from Molecular Simulations, Inc., with the DGII program, and graphical displays were printed out from the Insight molecular modeling system.

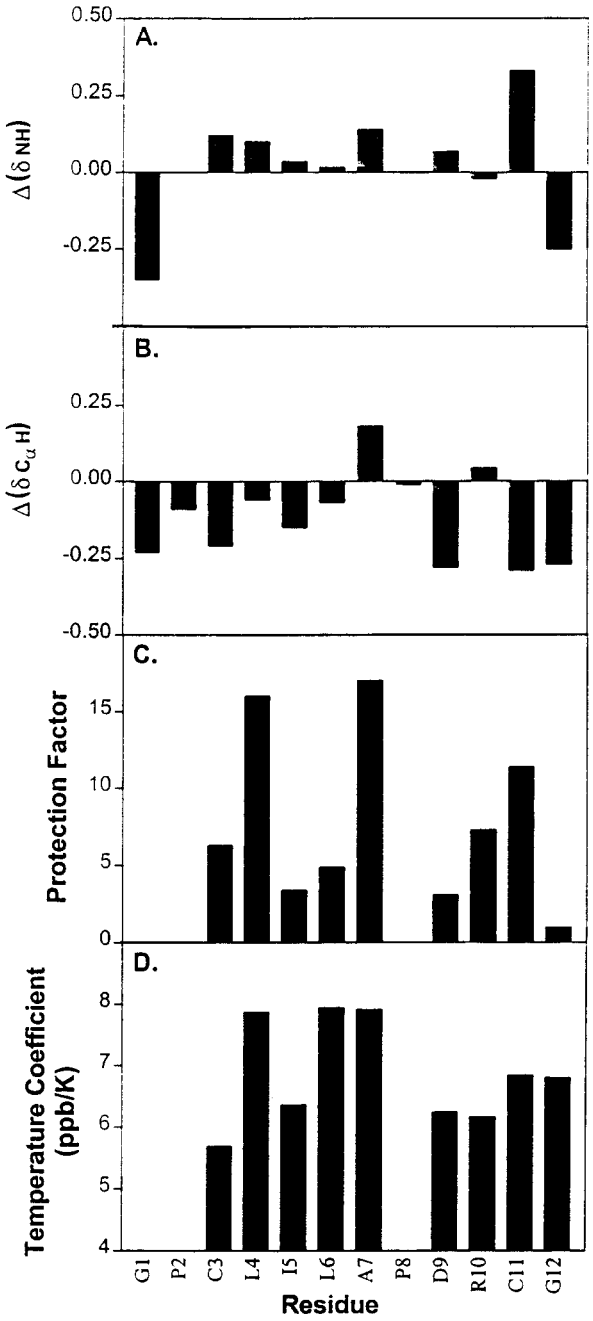

FIGURE 6: Summary of NMR data for peptide P1. Deviation of (A) NH and (B) CαH chemical shifts from random coil values (61). (C) Protection factors obtained from deuterium exchange studies, using the procedure of Bai et al. (50). (D) Temperature coefficients for amide protons, based on DQF-COSY spectra obtained at 279.9, 287.2, 294.6, and 302.0 K.

shown for the best 15 structures in Figure 9A,B, respectively. The thioether turn is moderately well-defined, with a Cα−Cα separation between the amino- and carboxy-terminal cysteines of 4.9 ± 0.8 Å for the 15 structures in Figure 9A. The Ala-(α-Me-Pro)-Asp-Arg turn region is more ordered. Since the distance between the carbonyl oxygen of alanine-7 and the amide hydrogen of arginine-10 is 2.2 ± 0.6 Å for the 15 structures in Figure 9B, there is most likely an *i* to *i*+3 hydrogen bond stabilizing this turn. This hydrogen bond was not forced explicitly as a constraint or implicitly through the use of a force field, but rather is purely a result of the ROE and covalent bond constraints. The ϕ/ψ angles for the *i*+1 (α-Me-Pro-8) and *i*+2 (Arg-9) residues in the 15 structures in Figure 9B fall into 2 major families (Table 2). That these fall into or close to allowed regions of the Ramachandran plot was encouraging, since no molecular mechanics force field was used in generating these structures. Although the geometry around the glycine-1/proline-2 peptide bond could not be established unambiguously because of spectral overlap, the Ala-7/α-Me-Pro-8 peptide bond is clearly trans. ROEs were observed between the α-Me-Pro-8 δH and both the alanine-7 αH and the alanine-7 βH. Conversely, no ROEs were observed between the α-methyl of α-Me-Pro-8 and the alanine-7 αH or NH.

Modeling the Role of the α*-Methyl in Proline-8.* The turn region comprised of trans α-methyl proline and flanking alanine and aspartate residues, in the solution structure of LJP 685, changed very little after minimization (Figure 9C, left side) in water. The methyl groups on alanine-7 and α-methyl proline-8 are far apart, so they cannot interact. Peptide P1 is very similar in sequence to LJP 685, yet its central proline is in the cis configuration. To better understand why the α-methyl proline induced a trans peptide bond in LJP 685, a methyl group was modeled onto the cis proline in the solution structure of peptide P1 (in addition to subtle changes elsewhere in the molecule, as described under Materials and Methods). After minimization in water, it was found that the methyl of alanine-7 was so close to the α-methyl of proline-8, with a carbon−carbon distance of 3.6 Å, that the methyl protons would clash when they rotated. This modeled turn region, comprised of cis α-methyl proline, with flanking alanine and aspartate residues, is shown on the right in Figure 9C. The structures in Figure 9C were thus derived from the solutions structures of LJP 685 (left) and peptide P1 (right) which have the central proline in the trans and cis configurations, respectively.

DISCUSSION

Autoimmune anti-cardiolipin antibodies (ACA's) have been associated with recurrent thrombosis. Indeed, it is estimated that between 5 and 10% of strokes are associated with high ACA titers (*57*). ACA's are directed against β_2GPI (*2*, *3*), although the affinity for this antigen is poor unless it is bound to an anionic phospholipid surface. This effect is thought to be due to the unmasking of a cryptic epitope upon binding to the surface, and/or by the presentation of the antigen to the antibody in high density so that increased affinity is achieved through avidity. BIAcore titrations indicate that solution-phase β_2GPI binds to solid-phase ACA 6501 with a K_d of 1.4 μM (Figure 1C,D), but if ACA 6501 is soluble and β_2GPI is on the solid-phase support, then the K_d is 52 nM (Figure 1E,F). This 27-fold increase in affinity is from the avidity/entropic advantage of having the β_2GPI antigen effectively made multivalent by being attached to the BIAcore CM5 chip. That is, a 2:1 interaction effectively becomes a 2:2 interaction. For this reason, kinetic analysis of association is not appropriate (*55*). Obviously, the magnitude of the avidity effect will depend on the density at which antigen coats the chip surface. Attachment to the chip simulates the *in vivo* situation where β_2GPI is bound in high density to anionic phospholipid surfaces. However, the modified CM5 chip presents a very different chemical environment compared to the anionic phospholipid surface, so at least some of the affinity advantage of ACA binding to membrane-bound β_2GPI must come from avidity, and not

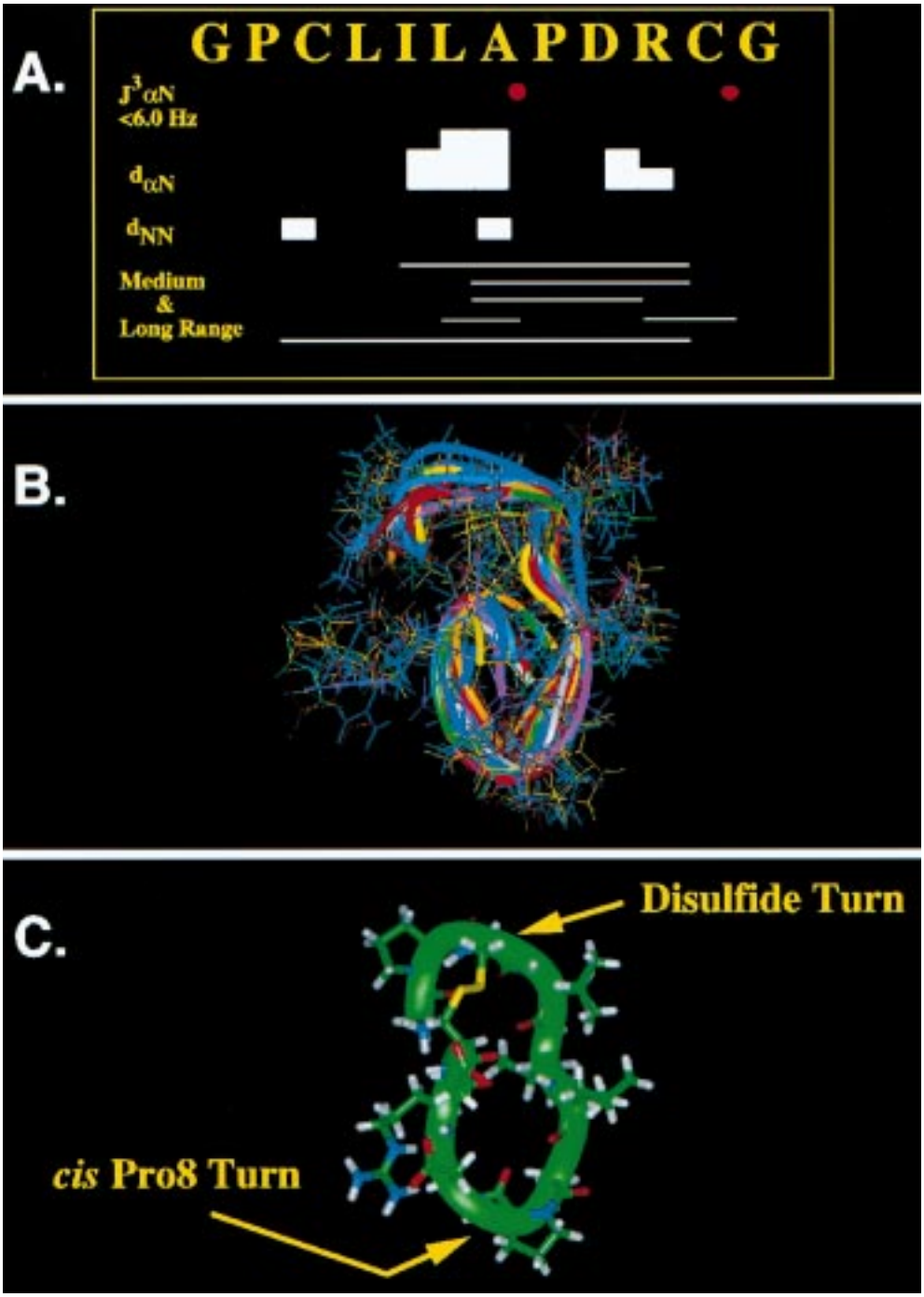

FIGURE 7: (A) Summary of NOE and coupling constant data used to calculate the solution structure of peptide P1. (B) Overlay of the 15 structures with lowest final error in the objective function, from the 50 structures calculated with DGII (MSI).[7] (C) Structure closest to the centroid for the ensemble of structures in (B).

merely revealing of a cryptic epitope because binding to the anionic surface induces a conformational change. The higher affinity observed for ACA 6501 binding to the recombinant versus the native β_2GPI (Figure 1A,B) could be a result of the faster and gentler purification of the recombinant protein using a nickel-chelation column (*31*).

Previously, 37 peptide mimotopes of the β_2GPI antigen were identified by phage library screening using ACA 6501 as the selecting antibody (*1*). The 2 peptide sequences that best represent the sequence motif of the 37 peptides, and have high affinity for ACA 6501, are characterized in this paper. Binding of peptide-phage to antibody is the key event in the selection process, and this binding has been monitored directly using surface plasmon resonance to detect (peptide P4)-phage binding to ACA 6501, attached to a BIAcore CM5 chip (Figure 2). Significant binding above background is observed at a phage concentration of 2×10^{11} pfu/mL.

In going from peptide, in the context of the pIII protein on phage, to a synthetic, isolated peptide, high-affinity binding to ACA 6501 is retained. Using fluorescence polarization direct binding titrations (Figure 3 and Table 1), the K_d was found to be 42 nM for ACA 6501 binding to peptide P4: $A^1G^2P^3C^4I^5L^6L^7A^8R^9D^{10}R^{11}C^{12}P^{13}G^{14}$, which is 40-fold tighter than the interaction with native soluble β_2GPI antigen. The DQF-COSY spectrum of the related peptide P2 (without alanine-1), which also has a proline carboxy

FIGURE 8: Overlay of the solution structures of peptide P1 (green carbon atoms) and LJP 685 (white carbon atoms). Each structure represents the centroid of structures calculated with distance geometry.

terminal to the last cysteine, has twice the expected number of cross-peaks in the fingerprint region (Figure 5A). But, if that carboxy-terminal proline is removed, the number of cross-peaks is cut in half (Figure 5B). Thus, the carboxy-terminal proline appears to be present in both the cis and trans configurations, with both configurations producing very different tertiary structures, as reflected in their different chemical shifts. Since peptide lacking this proline binds ca. 2-fold better to ACA 6501 (Figure 4 and Table 1), one or both of these two structures must have lower affinity for antibody. Another residue of interest is the first arginine, which when substituted with proline, comparing peptides P4 and P3, results in a 10-fold decrease in binding affinity for ACA 6501 (Figure 4 and Table 1). Interestingly, another peptide produced from phage library screening, peptide P2, has a proline rather than arginine in position 9, but also has a leucine for isoleucine substitution in position 5. The K_d for peptide P2 is 96 nM, very comparable to the 42 nM K_d for peptide P4, suggesting that the phage library screening must have selected for a non-β-branched amino acid in this position to somehow compensate for the adverse effects of the arginine-9 to proline-9 substitution.

The solution structure of peptide P1, a modified version of the phage selected peptide P4 with the central proline, has been determined. Deviations of chemical shifts from random coil are not large (Figure 6A,B), except for the CαH of alanine-7. Protection factor and temperature coefficient data show no compelling evidence for the presence of any hydrogen bonds (Figure 6C,D). The peptide P1 structure is fairly well-defined, with an all-atom rmsd of 2.13 $\pm$ 0.22 Å for the 15 best structures (Figure 7B). One turn is comprised of Ala-Pro-Asp-Arg, with the proline in the cis configuration, and the other turn contains the disulfide and leucine-4 (Figure 7C). The carboxy-terminal glycine is very flexible, since it contains the only amide with a positive NOE.

Modifications were made to peptide P1 in order to make it more metabolically stable, producing peptide LJP 685. The most significant peptidomimetic changes relative to peptide P1 are the replacement of the disulfide bond with a thioether linkage, and the replacement of the central turn proline with α-methyl proline. Previous literature had suggested that α-methyl proline may stabilize a type I β turn, and does increase antibody affinity for a proline-containing peptide that binds to antibodies against *Plasmodium falciparum* circumsporozoite protein (*58*). Other studies have shown that thioethers are structurally and functionally similar to disulfides (*28*, *30*). These changes had little effect on the binding affinity for ACA 6501, and the structure is also very similar to peptide P1 with an rmsd difference of only 1.37 Å, when comparing backbone atoms (Figure 8). The structure of LJP 685 is well-defined, with an all-atom rmsd of 2.82 $\pm$ 0.29 Å for the best 15, out of 100 structures. The thioether turn region is somewhat tightly defined with a Cα to Cα separation of 4.9 $\pm$ 0.8 Å in those 15 structures (Figure 9A). The α-methyl proline adopts the trans configuration, and this central Ala-(α-methyl-Pro)-Asp-Arg turn adopts a distorted type I turn conformation with a probable *i* to *i*+3 hydrogen bond between the carbonyl of alanine and the amide of arginine. The distance between the carbonyl oxygen of alanine-7 and the amide nitrogen of arginine-10 is 2.2 $\pm$ 0.6 Å for the 15 structures in Figure 9B, close to ideal for a hydrogen bond. This hydrogen bond was somewhat unexpected, since temperature coefficient data (not shown) gave no suggestion of any hydrogen bonding. This same *i* to *i*+3 hydrogen bonding pattern has been observed in the Asn-(α-methyl-Pro)-Asn-Ala motif (*58*). Although the B family of LJP 685 structures (Table 2) does not represent a classical turn, the A family of structures (Table 2) is most like a distorted type I turn (*59*), with ϕ/ψ angles for the *i*+2 position that deviate from the ideal. Previous reports suggest that the α-methyl proline group may stabilize type I β turns (*58*, *60*).

Modeling studies have been carried out starting from the LJP 685 structure with a trans proline-8, and the P1 structure with a cis proline-8, after addition of the α-methyl group to that proline, and other changes to make it the same composition and configuration as LJP 685 (see Materials and Methods). The LJP 685 structure shows no steric hindrance

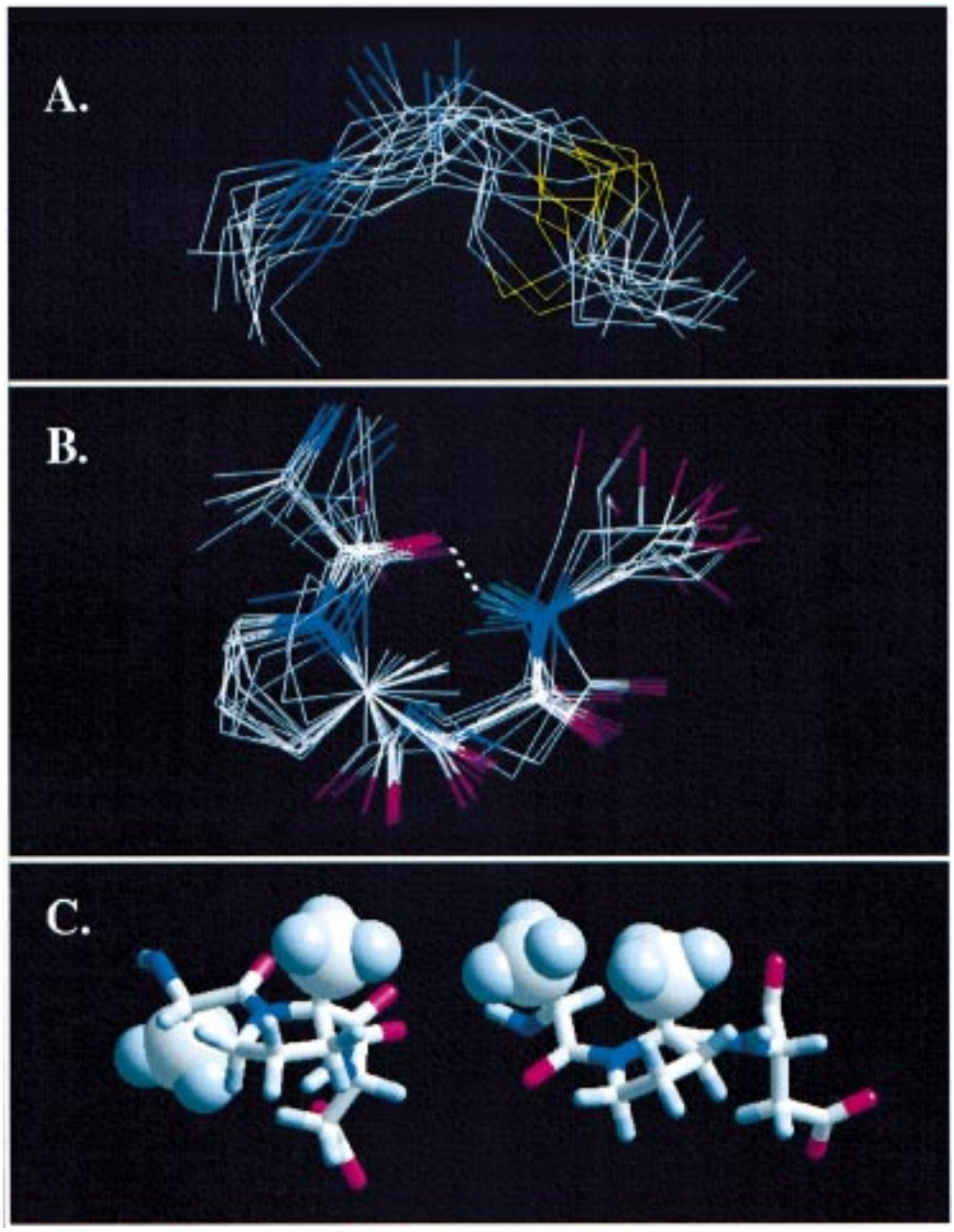

FIGURE 9: The 15 structures with lowest rmsd deviation from the centroid are shown from the set of 100 LJP 685 structures calculated with DGEOM. (A) Backbone and thioether linker atoms only are shown for the thioether turn region. The turn starts with isoleucine-4 on the left, followed by homocysteine-3 which is linked to cysteine-11 through the thioether bond. The glycine-1/proline-2 residues, which have been omitted, would have attached to the nitrogen at the top of the figure. (B) The tighter turn region at the other end of LJP 685 comprised of (from left to right) alanine-7, trans α-methyl proline-8, aspartate-9, and arginine-10. In addition to backbone atoms, the side chain of proline, the carbonyl oxygens, and the amide hydrogen of arginine are shown. The probable hydrogen bond between the carbonyl of alanine-7 and the amide of arginine-10 is shown with a dashed line. (C) The methyl groups are shown with CPK rendering in the alanine-7, α-methyl proline-8, aspartate-9 region. The left structure is LJP 685 (trans α-methyl proline) after minimization of the centroid NMR structure in water. The right structure is that of peptide P1 minimized in water, keeping the proline peptide bond cis, but adding an α-methyl group (in addition to subtle changes elsewhere in the molecule to give it to the atomic configuration of LJP 685).

Table 2: ϕ/ψ Angles for the LJP 685 Turn Comprised of Alanine-7, α-Methyl Proline-8, Aspartate-9, and Arginine-10

family	no. in family	ϕ (i+1)	ψ (i+1)	ϕ (i+2)	ψ (i+2)
A	6	-63 ± 3	-22 ± 7	-55 ± 3	-47 ± 11
B	7	-69 ± 9	32 ± 23	-120 ± 12	-37 ± 12

with the α-methyl of proline-8 (Figure 9C, left side), but there is a clear steric clash if a methyl is placed in the α position on cis proline-8 of the modified peptide P1 structure, even after minimization in water (Figure 9C, right side). The steric hindrance between the methyl of α-methyl proline and the β-methyl of the preceding residue may be a general phenomenon that will result in the preference for a trans peptide bond in peptides containing α-methyl proline. Similar effects have been suggested for the asparagine preceding an α-methyl proline (*58*).

In summary, LJP 685 is a high-affinity peptidomimetic version of an antibody-selected phage-displayed cyclic peptide that binds to an ACA. It is a fairly structured peptide

containing a distorted type I β turn, that must mimic the antigenic region on β_2GPI that is recognized by the selecting antibody. Although these peptides show no primary sequence homology to β_2GPI, they are antigen mimotopes since they can displace ACA 6501 from β_2GPI in competitive ELISA assays (*1*). LJP 685's high affinity is probably due in part to its tight cyclic structure, which avoids the entropic penalty that would be encountered by an antibody having to bind a flexible peptide (*19*). Thioether and α-methyl proline substitutions have proven to be structurally and functionally conservative substitutions in the design of this peptidomimetic molecule.

ACKNOWLEDGMENT

We thank Keith Cockerill for providing us with the (P4-peptide) phage and Professor Steve Krilis of St. George Hospital, Kogarah, Australia, for providing the BacPAK9 vector containing the cDNA for β_2GPI. We also thank Michael Weisman of the UCSD Medical Center, and Richard Furie of New York University and North Shore University Hospital, Manhasset, NY, who identified and aided in obtaining plasma from the patient used in this study.

REFERENCES

1. Kandiah, D., Sali, A., Sheng, Y., Victoria, E. J., Marquis, D., Coutts, S. M., and Krilis, S. A. (1998) *Adv. Immunol. 70*, 507−563.
2. Galli, M., Comfurius, P., Maassen, C., Hemker, H. C., De Baets, M. H., van Breda-Vriesman, P. J. C., Barbui, T., Zwaal, R. F. A., and Bevers, E. M. (1990) *Lancet 335*, 1544−1547.
3. McNeil, H. P., Simpson, R. J., Chesterman, C. N., and Krilis, S. A. (1990) *Proc. Natl. Acad. Sci. U.S.A. 87*, 4120−4124.
4. Hughes, G. R. V., Harris, E. N., and Gharavi, A. E. (1986) *J. Rheumatol. 13*, 486-489.
5. Harris, E. N. (1991) *The Anti-Phospholipid Syndrome*: *An Introduction* (Harris, E. N., Exner, T., Hughes, G. R. V., and Asherson, R. A., Eds.) pp 373−376, CRC Press, Boca Raton.
6. Schultze, H. E., Heide, K., and Haupt, H. (1961) *Naturwissenschaften 23*, 719.
7. Polz, E., and Kostner, G. M. (1979) *FEBS Lett. 102*, 183−186.
8. Matsuura, E., Igarashi, Y., Yasuda, T., Triplett, D. A., and Koike, T. (1994) *J. Exp. Med. 179*, 457−462.
9. Roubey, R. A. S. (1994) *Blood 84*, 2854−2867.
10. Igarashi, M., Matsuura, E., Yoshiko, I., Nagae, H., Ichikawa, K., Triplett, D. A., and Koike, T. (1996) *Blood 87*, 3262−3270.
11. Hunt, J., and Krilis, S. (1994) *J. Immunol. 152*, 653−659.
12. Lozier, J., Takahashi, N., and Putnam, F. W. (1984) *Proc. Natl. Acad. Sci. U.S.A. 81*, 3640−3644.
13. Jones, D. S., Barstad, P. A., Field, M. J., Hachmann, J. P., Hayag, M. S., Hill, K. W., Iverson, G. M., Livingston, D. A., Palanki, M. S., Tibbetts, A. R., Yu, L., and Coutts, S. M. (1995) *J. Med. Chem. 38*, 2138−2144.
14. Khamashta, M. A., Cuadrado, M. J., Mujic, F., Taub, N. A., Hunt, B. J., and Hughes, G. R. V. (1995) *N. Engl. J. Med. 332*, 993−997.
15. Asherson, R. A., Chan, J. K. H., Harris, E. N., Gharavi, A. E., and Hughes, G. R. V. (1985) *Ann. Rheum. Dis. 44*, 823−825.
16. Spinnato, J. A., Clark, A. L., Pierangeli, S. S., and Harris, E. N. (1995) *Am. J. Obstet. Gynecol. 172*, 690−694.
17. Smith, G. P., and Scott, J. K. (1993) *Methods in Enzymology* (Abelson, J. N., and Simon, M. I., Eds.) p 228, Academic Press, New York.
18. Schellekens, G. A., Lasonder, E., Feijlbrief, M., Koedijk, D. G. A. M., Drijfhout, J. W., Scheffer, A.-J., Welling-Wester, S., and Welling, G. W. (1994) *Eur. J. Immunol. 24*, 3188−3193.
19. Giebel, L. B., Cass, R. T., Milligan, D. L., Young, D. C., Arze, R., and Johnson, C. R. (1995) *Biochemistry 34*, 15430−15435.
20. Katz, B. (1995) *Biochemistry 34*, 15421−15429.
21. Westhof, E., Altschuh, D., Moras, D., Bloomer, A. C., Mondragon, A., Klug, A., and van Regenmortel, M. H. V. (1984) *Nature 311*, 123−126.
22. Novotny, J., Handschumacher, M., Haber, E., Bruccoleri, R., Carlson, W. B., Fanning, D. W., Smith, J. A., and Rose, G. D. (1986) *Proc. Natl. Acad. Sci. U.S.A. 83*, 226−230.
23. Tainer, J. A., Getzoff, E. D., Alexander, H., Houghton, R. A., Olson, A. J., Lerner, R. A., and Hendrickson, W. A. (1984) *Nature 312*, 127−134.
24. Dyson, H. J., and Wright, P. E. (1995) *FASEB J. 9*, 37−42.
25. Dyson, H. J., and Wright, P. E. (1991) *Annu. Rev. Biophys. Biophys. Chem. 20*, 519−538.
26. Dyson, H. J., Lerner, R. A., and Wright, P. E. (1988) *Annu. Rev. Biophys. Biophys. Chem. 17*, 305−324.
27. Qabar, M., Urban, J., Sia, C., Klein, M., and Kahn, M. (1996) *IL Farmaco 51*, 87−96.
28. Katz, B. A., Johnson, C. R., and Cass, R. T. (1995) *J. Am. Chem. Soc. 117*, 8541−8547.
29. Moore, G. J., Smith, J. R., Baylis, B. W., and Matsoukas, J. M. (1995) *Adv. Pharmacol. 33*, 91−141.
30. Mayer, J. P., Heil, J. R., Zhang, J., and Munson, M. C. (1995) *Tetrahedron Lett. 36*, 7387−7390.
31. Iverson et al. (1998), in preparation.
32. Zebedee, S. L., Barbas, C. F., Hom, Y.-L., Caothien, R. H., Graff, R., DeGraw, J., Pyati, J., LaPolla, R., Burton. D. R., Lerner, R. A., and Thornton, G. B. (1992) *Proc. Natl. Acad. Sci. U.S.A. 89*, 3175−3179.
33. Scott, J. K., and Smith, G. P. (1990) *Science 249*, 386−390.
34. Wellings, D. A., and Atherton, E. (1997) *Methods Enzymol. 289*, 44−67.
35. Jones, D. S. (1998), in preparation.
36. Harris, E. N. (1990) *Br. J. Haematol. 74*, 1−9.
37. Pengo, V., Thiagarajan, P., Shapiro, S. S., and Heine, M. J. (1987) *Blood 70*, 69−76.
38. Biosensor (1994) in *BIAapplications Handbook*, Pharmacia Biosensor AB, Uppsala, Sweden.
39. Wells, A. F., Miller, C. E., and Nadel, M. K. (1966) *Appl. Microbiol.* 271−275.
40. Sem, D. S., and McNeeley, P. A. (1998), in preparation.
41. Fersht, A. R. (1985) in *Enzyme Structure and Mechanism*, W. H. Freeman, New York.
42. Bodenhausen, G., Vold, R. L., and Vold, R. R. (1980) *J. Magn. Reson. 37*, 93−106.
43. Marion, D., and Wüthrich, K. (1983) *Biochem. Biophys. Res. Commun. 113*, 967−974.
44. Rance, M., Sorenson, O. W., Bodenhausen, G., Wagner, G., Ernst, R. R., and Wüthrich, K. (1983) *Biochem. Biophys. Res. Commun. 117*, 479−485.
45. Bax, A., and Davis, D. G. (1985) *J. Magn. Reson. 63*, 207−213.
46. Bodenhausen, G., Kogler, H., and Ernst, R. R. (1984) *J. Magn. Reson. 58*, 370−388.
47. Bax, A., and Davis, D. G. (1985) *J. Magn. Reson. 65*, 355−360.
48. Delaglio, F., Grzesiek, S., Vuister, G. W., Zhu, G., Pfeifer, J., and Bax, A. (1995) *J. Biomol. NMR 6*, 277−293.
49. Marion, D., Ikura, M., and Bax, A. (1989) *J. Magn. Reson. 84*, 425−430.
50. Bai, Y., Milne, J. S., Mayne, L., and Englander, S. W. (1993) *Proteins*: *Struct., Funct., Genet. 17*, 75−86.
51. Guenot, J., and Kollman, P. A. (1992) *Protein Sci. 1*, 1185−1205.
52. Kördel, J., Skelton, N. J., Akke, M., and Chazin, W. J. (1993) *J. Mol. Biol. 231*, 711−734.
53. Kördel, J., Pearlman, D. A., and Chazin, W. J. (1997) *J. Biomol. NMR 10*, 231−243.
54. Weiner, S. J., Kollman, P. A., Case, D. A., Singh, U. C., Ghio, C., Alagona, G., Profeta, S., and Weiner, P. (1984) *J. Am. Chem. Soc. 106*, 765−784.

55. Bowles, M. R., Hall, D. R., Pond, S. M., and Winzor, D. J. (1997) *Anal. Biochem. 244*, 133−143.
56. Schuck, P. (1997) *Annu. Rev. Biopys. Biomol. Struct. 26*, 541−566.
57. Antiphospholipid Antibodies in Stroke Study (APASS) group (1997) *Neurology 47*, 91−94.
58. Bisang, C., Weber, C., Inglis, J., Schiffer, C. A., van Gunsteren, W. F., Jelesarov, I., Bosshard, H. R., and Robinson, J. A. (1995) *J. Am. Chem. Soc. 117*, 7904−7915.
59. Wilmot, C. M., and Thornton, J. M. (1988) *J. Mol. Biol. 203*, 221−232.
60. Hinds, M. G., Welsh, J. H., Brennand, D. M., Fisher, J., Glennie, M. J., Richards, N. G. J., Turner, D. L., and Robinson, J. A. (1991) *J. Med. Chem. 34*, 1777−1789.
61. Wüthrich, K. (1986) in *NMR of Proteins and Nucleic Acids*, John Wiley, New York.

BI9807207